Flexible UV-Ozone-Modified Carbon Nanotube Electrodes for Neuronal Recording

By *Hui-Lin Hsu, I-Ju Teng, Yung-Chan Chen, Wei-Lun Hsu, Yu-Tao Lee, Shiang-Jie Yen, Huan-Chieh Su, Shih-Rung Yeh, Hsin Chen,* and *Tri-Rung Yew**

Neurophysiologists have used sharpened metal electrodes to electrically stimulate neuronal activities to investigate the physiological functions of the brain. Moreover, they employed this electrical stimulation to treat diseases such as Parkinson's disease, dystonia, and chronic pain.[1–5] As neurons utilize electrical potential difference between their cell membranes to transmit electrical signals, this particular way of communication enables us to record the neuronal activity extracellularly or intracellularly. For the extracellular recording approach, the electrodes are positioned intimately next to neuron cells to record and to stimulate their electrical activity by capacitive coupling. The coupling efficacy of these electrical recordings or interventions depends significantly on the selectivity, sensitivity, charge-transfer characteristics, long-term chemical stability, and interfacial impedance between electrodes and target tissue.[5,6]

The most common approach to further investigate the functional behavior of neurons, is using Si-based multi-microelectrode probes fabricated by the micro-electromechanical system (MEMS) method to replace the conventional electrodes (Ag/AgCl) in the aspect of device-structure improvement and scaling down device sizes.[7–11] However, Si-based MEMS electrodes are extremely rigid and cannot be deformed inside the organs; therefore, the recorded positions are easily shifted and the target tissues are consequently damaged when the animals are in motion. This will become an obstacle in future long-term implantation and real-time recording applications. An alternative method is the use of flexible electrodes presented by several groups.[12–16] The authors utilized soft materials, such as poly(dimethylsiloxane), SU-8 epoxy-based negative photoresist, and polyimides, to fabricate microelectrodes that can deform while being attached to the tissues and that can also be fabricated into small-scale devices using MEMS methods.

Not only would rigid Si-based MEMS probes damage target tissues, the reduced electrode size also resulted in a significantly increase in impedance that may degrade recording sensitivity and limit the stimulating current deliverable through an electrode. In order to resolve above issues, the impedance of the electrode must be as low as possible.[5,6] Carbon nanotubes (CNTs) exhibit intrinsically large surface areas (700–1000 $m^2 g^{-1}$), high electrical conductivity, and intriguing physicochemical properties.[17–21] Most importantly, CNTs are chemically inert and biocompatible.[22–24] Based on the above, the promising advantages of flexible substrates and CNTs lead the attempt of fabricating CNTs directly on flexible substrates as microelectrodes for neuronal recording.

In this work, the feasibilities of growing CNTs on flexible polyimide substrates at low temperatures (400 °C) by catalyst-assisted chemical vapor deposition (CVD) and utilizing the above devices (see the schematic image in Fig. 1a and the photo in Fig. 1b) as electrodes for extracellularly neuronal recording were investigated. The electrical enhancement (by UV-ozone exposure), biocompatibility (by neuron cell cultures), long-term usage and adhesion, and the detection of action-potential signals on crayfish (using flexible UV-ozone-modified CNT electrodes) were examined.

After a series of process optimizations, the 5-nm Ni-catalyst layer and C_2H_2 (60 sccm)/H_2 (10 sccm) process gases at 5 Torr were found to be the optimum CNT growth parameters in this work. Besides, the Au layer could facilitate CNT growth. Figure 1c shows that CNTs have been grown on the polyimide substrate with Au layer, while not on that without Au layer (the inset). The high-resolution transmission electron microscopy (HRTEM) image (Fig. 1d) further confirms the successful syntheses of multi-walled carbon nanotubes (MWCNTs) at 400 °C or even down to 350 °C with H_2 plasma pretreatment prior to the CVD processing. As shown in the Supporting Information (Fig. S1a),

[*] Prof. T.-R. Yew, H.-L. Hsu, S.-J. Yen, H.-C. Su
Department of Materials Science and Engineering
National Tsing-Hua University (NTHU)
101, Sec. 2, Kuang-Fu Road
Hsinchu 30013 (Taiwan)
E-mail: tryew@mx.nthu.edu.tw
I.-J. Teng
Department of Materials Science and Engineering
National Chiao-Tung University
Hsinchu 30013 (Taiwan)
Y.-C. Chen, Prof. H. Chen
Institute of Electronics Engineering, NTHU
Hsinchu 30013 (Taiwan)
W.-L. Hsu
Department of Life Science, NTHU
Hsinchu 30013 (Taiwan)
Y.-T. Lee
Institute of NanoEngineering and MicroSystems, NTHU
Hsinchu 30013 (Taiwan)
Prof. S.-R. Yeh
Institute of Molecular Medicine, NTHU
Hsinchu 30013 (Taiwan)

DOI: 10.1002/adma.200903413

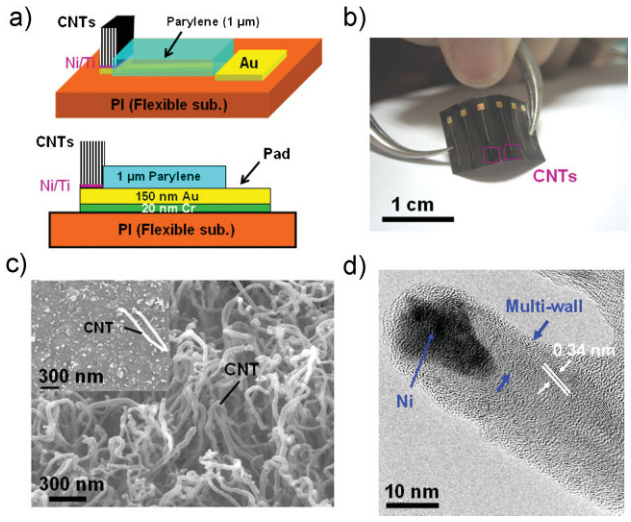

Figure 1. a) A schematic side and cross-section view and b) a photo, of flexible CNT electrode devices. c) Figure and inset show SEM images of CNTs grown on Ni (5 nm)/Ti (20 nm)/Au (150 nm)/Cr (20 nm) and Ni (5 nm)/Ti (20 nm) on polyimide, respectively.

the length of MWCNTs is controllable and increases approximately linearly with the increase of growth time (growth rate ~77 nm min^{-1}). Besides, the impedance decreases linearly and the capacitance increases linearly with the increase of CNT length (Fig. S1b). This approach shows advantages of being able to integrate patterned CNTs directly onto flexible substrates for future flexible electronics applications that require low growth temperature.

The interfacial properties between CNTs and the electrolyte, which play an important role in neuronal signal detection, can be improved by UV-ozone exposure. As the duration of UV-ozone exposure increases, the impedance per unit area of the CNT electrodes decreases. Besides, the surface wettability of CNTs is changed from superhydrophobic to hydrophilic (Fig. 2a), as shown by the contact angles of 160°, 98°, and smaller than 5° (insets of Fig. 2a) measured from the CNTs with UV-ozone exposure for 0, 10, and 40 min, respectively. The impedance per unit area drops more than one order of magnitude for CNTs after 20 min UV-ozone exposure and reaches a saturation value (~30 kΩ mm^{-2}) after UV-ozone exposure for 40 min or longer. Besides, the interfacial capacitance per unit area (Fig. 2b), derived from cyclic voltammetry (CV) data, increases from 5.7×10^{-8} F mm^{-2} for as-grown CNTs to greater than 10^{-6} F mm^{-2} for the CNTs subjected to more than 10 min UV-ozone exposure. Benefiting from lower interfacial impedance and higher capacitance, as above, UV-ozone modified CNT electrodes can provide better charge-transfer capability and consequently facilitate their application for neuronal recording.

In addition, the CNT/electrolyte interface can be modeled electrically as a resistor and a capacitor in parallel.[25–27] The resistive impedance, Z_R ($Z_R = R$, Fig. 2c), was comparable to capacitive impedance, Z_C ($Z_C = 1/(2\pi fC)$, Fig. 2d), where R, f, and C are resistance, frequency, and capacitance, respectively, implying that the CNT electrode transmits signals through both capacitive and resistive conduction. This differs from the previous reports which suggested that only capacitive conduction dominated.[25,28] More interestingly, both Z_C and Z_R of the 40-min UV-ozone-modified CNTs were reduced to about 1/50 of their individual values of as-grown CNTs, i.e., Z_C was reduced from 1340 to 22 Ω mm^{-2} and Z_R from 25800 to 468 Ω mm^{-2} at 1 kHz. The resistive characteristic is very crucial to record equilibrium membrane potentials and to deliver direct-current stimuli in intracellular recording.

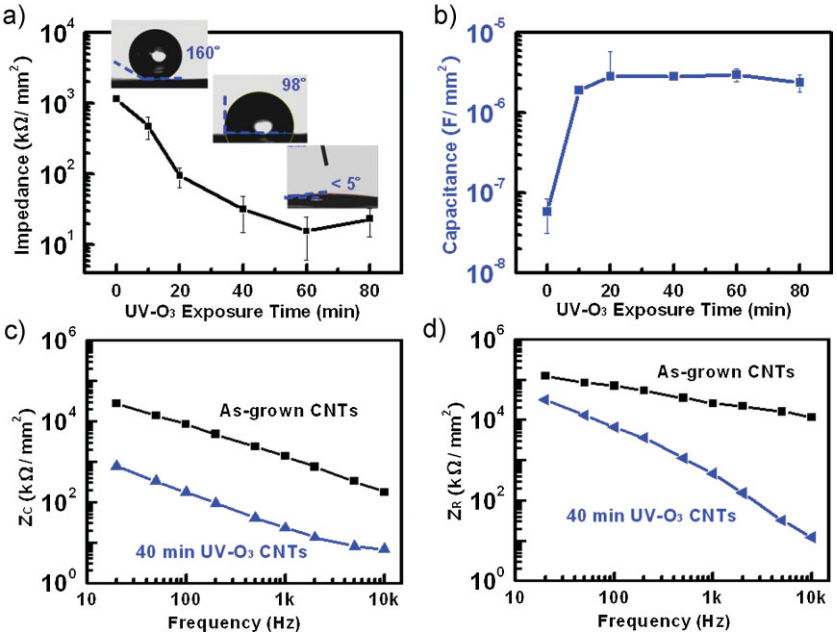

Figure 2. Interfacial impedance (a) and capacitance (b) of CNT electrodes per unit area as a function of UV-ozone exposure time. c) Z_C and d) Z_R of as-grown and 40-min UV-ozone-modified CNTs.

To further investigate chemical concentration changes qualitatively on CNTs, X-ray photoelectron spectroscopy (XPS) analyses were performed. Figure 3a shows that the C1s peak intensity is reduced and a high binding energy shoulder appears for the UV-ozone modified CNTs, while the O1s spectra in Figure 3b show that intensities from oxygen-related bonds increase with UV-ozone exposure time, suggesting the reduction of carbon-related bonds and the formation between carbon–oxygen bonds. The Gaussian decompositions of Figure 3a are shown in Figure 3c–e for more detailed analyses, all exhibiting five peaks at 284.6, 285.3, 286.2, 287.6, and 289.4 eV, which are attributed to sp^2-hybridized C=C (graphite), sp^3-hybridized C–C (diamond-like), C–O, C=O, and O–C=O bonds,[29–32] respectively. Besides, the relative percentages of C–O, C=O, and O–C=O bonds increase with the increment of UV-ozone exposure time, and the major bonding form between C and O is

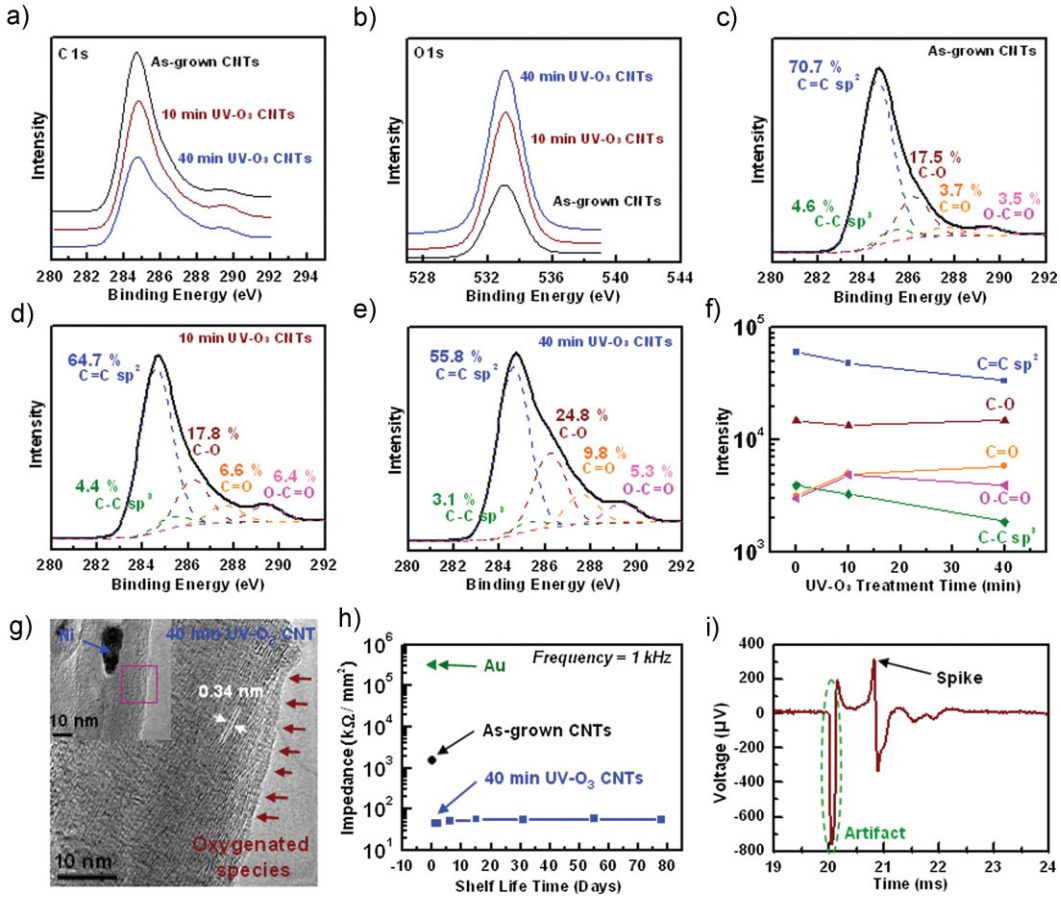

Figure 3. a) C1s and b) O1s spectra of as-grown, and 10- and 40-min UV-ozone-modified CNTs. Gaussian decompositions of as-grown CNTs (c) and CNTs after UV-ozone exposure for 10 min (d) and 40 min (e). f) Trend charts of C=C, C−C, C−O, C=O, and O−C=O bond intensities on CNTs as a function of UV-ozone exposure time. g) HRTEM image of a 40-min UV-ozone-modified CNT. h) Impedance per unit area of UV-ozone-modified CNT electrodes versus shelf life time in comparisons with Au and as-grown CNT electrodes. i) Detection of neuronal extracellular activities using UV-ozone modified flexible CNT electrodes; spikes evoked by electrical stimulation (artifact) are observed.

the C−O bond. The trend charts (Fig. 3f) show that the total intensity of C−O, C=O, and O−C=O bonds for UV-ozone-modified CNTs is higher than that of as-grown CNTs and increases with exposure time. This is consistent with the O1s spectra (Fig. 3b), although some slight deviation is observed in the trends of individual changes of C−O, C=O, and O−C=O bonds, possibly due to the scattering of physically absorptive O-contained species. The HRTEM image of the 40-min UV-ozone-modified CNT (Fig. 3g and its inset) show that the diameter and morphology are not varied significantly compared to that of as-grown CNTs (Fig. 1d). However, the graphitization structure of the outermost graphene shells is disrupted and discontinuous, suggesting the formation of C−O, C=O, and O−C=O bonds by UV-ozone exposure. Above results suggest that the improvement of interfacial resistive and capacitance characteristics (Fig. 2) is primarily contributed by the incremental C−O, C=O, and O−C=O bonds, which chemically anchor H_2O molecules via intermolecular bonding[33,34] and enhance the CNT/electrolyte interfacial contact and reaction.

The durability and adhesion tests of UV-ozone-modified flexible CNT electrodes were conducted. The interfacial impedance between as-grown CNTs and 3 M KCl solution was lower than that between Au and 3 M KCl solution by more than two orders of magnitude, and it was further reduced by more than one order of magnitude as the CNTs were treated by 40-min UV-ozone exposure for surface functionalization (Fig. 3h). It also shows negligible impedance change for flexible UV-ozone-modified CNT electrodes stored in air at ambient conditions during three months tracking (Fig. 3h). Furthermore, adhesion tests only show a negligible impedance change of CNT electrodes after ultrasonication in 3 M KCl solution for up to 120 s or inserting into quasi-neuron tissue (Agar gel) for 50 times. It can be inferred that the adhesion between the CNTs and the Ti layers is good. Above results on durability and adhesion tests imply the feasibility of using flexible UV-ozone-modified CNT electrodes fabricated in this work for long-term neuronal recording applications.

The capability of flexible UV-ozone-modified CNT electrodes in detecting neuronal activities extracellularly was demonstrated (Fig. 3i). Flexible CNT electrodes were employed to record the action potential of lateral giant (LG) neurons in the last abdominal ganglia of crayfish (*Procambarus clarkia*) in phosphate buffered

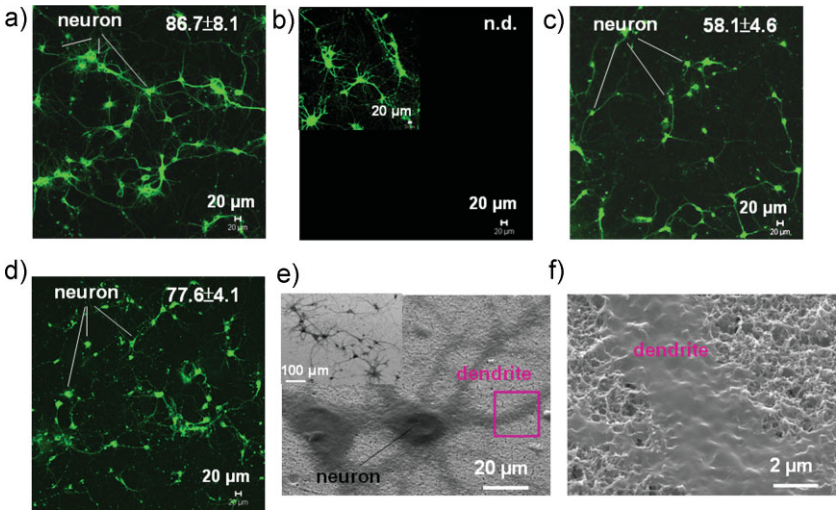

Figure 4. Fluorescent images of neuron cells cultured on control glass (a), as-grown CNTs (b), and UV-ozone-modified CNTs for 10 min (c) and 40 min (d). e,f) SEM images of Hippocampal neuron cells cultured on the same CNTs as (d).

saline (PBS). LG neurons received excitatory inputs from the nerves that innervated hairs on the tail fan. A bipolar electrode was placed onto the surface of the nerves, and two recording electrodes, a CNT electrode, and a suction pipette were attached tightly to the LG axon that was located on the dorsal surface of the nerve cord. A LG spike and several spikes following the LG spike were evoked by a 0.15 ms electrical stimulation (artifact in Fig. 3i) on the nerves. According to Figure 3i, the flexible UV-ozone-modified CNT electrodes were able to detect action potentials (APs) of lateral giant (LG) neurons and the recorded peak-to-peak magnitude of stimulated action potentials is 647 μV. The signal-to-noise ratio was about 150, which was obtained by dividing the peak-to-peak amplitude of the spike by the base line of the recording trace for UV-ozone-modified CNT electrodes with a pad area of 3600 μm^2. Comparison to the signal-to-noise ratios of about 122 measured by traditional suction pipettes and about 36 by Au electrodes, which served as references under the same setup, suggests that the performance of UV-ozone modified CNT electrodes can be referred as good as traditional suction pipettes or better than Au electrodes in extracellular recording. However, as the amplitude of the signals in extracellular recordings is dependent on the distance between the neuron and the electrodes, further precise control on the distance is required for statistical sensitivity comparisons, although the distance has been kept as constant as possible for the above neuron recordings.

Biocompatibility tests of CNT electrodes were also conducted (Fig. 4a–d). The neuron cells were aggregated severely on the certain region of as-grown CNTs (inset of Fig. 4b), while no neurons cells or neurite outgrowth branches were observed on the majority region (Fig. 4b). On the other hand, higher neuron-cell densities with homogeneous neuronal distribution can be observed at the increased duration of UV-ozone exposure, i.e., (58.1 ± 4.6) and (77.6 ± 4.1) mm^{-2} on 10-min (Fig. 4c) and 40-min (Fig. 4d) UV-ozone-modified CNTs, respectively, although slightly less than that on control glass ((86.7 ± 8.1) mm^{-2}) (Fig. 4a). From scanning electron microscopy (SEM) images of neurons cultured on the 40-min UV-ozone-modified CNT substrates (Fig. 4e and f), a promising adhesion between the neuron cells or neurite outgrowth branches and the UV-ozone- modified CNTs can be derived. This indicates that UV-ozone exposure can enhance the poly-L-lysine (PLL) attachment on CNTs and promote animated neuron and neurite growth in close contact with CNTs, suggesting good biocompatibility of UV-ozone-modified CNT electrodes. The enhancement of PLL attachments on UV-ozone modified CNTs is suspected to be attributed to the hydrophilic characteristics of CNTs after UV-ozone treatment according to contact-angle measurements, as PLL tends to attach to the hydrophilic surface, as reported.[35–37]

In summary, the feasibility of growing CNTs on polyimide substrates at low temperatures ($\leq$400 °C) as electrodes for extracellularly neuronal recording has been demonstrated. Besides, the UV-ozone exposure proposed in this work provides an easy, simple, and low-cost route to functionalize CNTs by inducing the formation of C−O, C=O, and O−C=O moieties on the outermost surface of CNTs and changing them to hydrophilic. This can enhance the electrical charge-transfer characteristics and the electrochemical properties of CNT electrodes significantly, attributed to the 50-fold impedance reduction and over 10 times increase in interfacial-capacitance. Furthermore, the flexible CNT electrodes were found to exhibit not only capacitive but also resistive characteristics. Besides, results on cell-cultures indicate good biocompatibility of UV-ozone-modified CNTs substrates for neuronal growth. Furthermore, the good durability and good adhesion with polyimide substrates suggest that the flexible UV-ozone modified CNT electrodes fabricated in this work are promising candidates for long-term neuronal-recording applications.

Experimental

Flexible CNT Electrode Fabrication: Kapton HPP-ST 125-μm polyimide films were adopted as flexible substrates, which were washed for 10 min with isopropyl alcohol and for further 10 min with deionized (DI) water sequentially using ultrasonication, followed by baking at 60 °C in air for 10 min. A 20-nm Cr adhesion layer and a 150-nm Au interconnect layer were deposited by electron-beam (e-beam) evaporation via a shadow-mask patterning method in sequence. A 20-nm Ti adhesion and a Ni catalyst layers for CNT growth were then deposited sequentially using a second shadow mask. Various-size Ni/Ti square pads (3600, 10000, 22500, and 40000 μm^2) were used to quantify the electrical properties of CNTs. The CNTs were synthesized using Ni as a catalyst and C_2H_2/H_2 as process gases at 350–450 °C. The gas-flow rate, process pressure, growth temperature, and growth time were investigated to optimize the quality and density of the CNTs on the polyimide substrates. Following the CNT syntheses, a 1-μm biocompatible poly(*para*-xylylene) (parylene) insulator layer [38] was thermally deposited on the Au layer, leaving only CNT pads exposed. Finally, the CNT electrodes were subjected to UV-ozone exposure using a UVO-Cleaner system (Jelight Company Inc, Irvine, CA, USA) at an intensity of 25–35 mW cm^{-2} and a wavelength of 254 nm.

Instrumentation: SEM (JEOL 6500) and HRTEM (JEOL JEM-2010) were employed to observe the morphology and structure of CNTs. Frequency-dependent changes in the impedance of flexible CNT electrodes were characterized by an Aligent 4284A system, where 10 mV sinusoidal signals at 20 Hz–10 kHz were applied to CNT electrodes in 3 M KCl solution using a Ag/AgCl coil as a reference electrode. Besides, CV measurements were conducted to determine the electrochemical properties of flexible CNTs electrodes. Each data point in this work was obtained from at least 3 samples ($n = 3$) and 3 measurements per sample. The surface wettability of CNTs was measured by a contact-angle measurement system. Moreover, XPS was used to characterize the chemical functionalization of CNT surfaces.

Neuronal Signal Detection: Electrophysiological recording was performed according to procedures described previously [39–40]. A pair of bipolar electrodes fabricated from Teflon-coated silver wires (70 μm in diameter; A-M systems, Carlsborg Washington) was placed onto the sensory nerves, and electrical shocks (1.5–3 V, 0.15 ms duration) were delivered to evoke LG spikes. A suction pipette filled with crayfish saline, a Au electrode, and a CNT electrode were placed onto the LG axon for spike recording. Recorded voltages were digitized at 500 kHz by a PCI-6251 DA/AD converter card (National Instruments, Austin, TX, USA). Crayfish was anesthetized in a 4 °C water bath, and the nerve cord was dissected and pinned dorsal-side up on Sylgard 184 (Dow Corning, Midland, Michigan, USA) in a Petri dish. The preparation was carried out in crayfish saline (Van Harreveld, 1936) containing 210 mM NaCl, 15 mM $CaCl_2$, 5.4 mM KCl, 2.6 mM $MgCl_2$, and 5 mM HEPES (all purchased from Sigma–Aldrich, St. Louis, MO, USA) at pH 7.4.

Neuron-Cell Cultures: Before culturing neuron cells, all materials were subjected to a sterilization process, where the substrates were immersed in alcohol for 30 min followed by rinsing in DI water 3 times. Morphologies of neurons and neurite outgrowth branches were observed after cell culturing for 16 days using confocal fluorescent microscopy with a 488-nm excitation wavelength and using β-III-tubulin as a cell marker. For each fluorescent image in the biocompatibility tests, at least three randomly selected areas (each with an area of 0.7 mm^2) per sample (area 1 cm^2) on three samples of each cell culture were monitored.

Acknowledgements

This work was supported by National Science Council under project numbers NSC 96-2627-E-007-002. The authors thank Professor F. M. Pan in the MSE department at NCTU for very valuable discussions on XPS analysis and the facility support from CNMM at NTHU. Supporting Information is available online from Wiley InterScience or from the author.

Received: October 10, 2009
Revised: November 21, 2009
Published online: March 30, 2010

[1] L. R. Hochberg, M. D. Serruya, G. M. Friehs, J. A. Mukand, M. Saleh, A. H. Caplan, A. Branner, D. Chen, R. D. Penn, J. P. Donoghue, *Nature* **2006**, *442*, 164.
[2] D. M. Taylor, S. I. Tillery, A. B. Schwartz, *Science* **2002**, *296*, 1829.
[3] J. K. Chapin, K. A. Moxon, R. S. Markowitz, M. Nicolelis, *Nat. Neurosci.* **1999**, *2*, 664.
[4] A. B. Schwartz, X. T. Cui, D. J. Weber, D. W. Moran, *Neuron* **2006**, *52*, 205.
[5] G. E. Loeb, R. A. Peck, J. Martyniuk, *J. Neurosci. Methods* **1995**, *63*, 175.
[6] D. A. Robinson, *Proc. IEEE* **1968**, *56*, 1065.
[7] F. Patolsky, B. P. Timko, G. Yu, Y. Fang, A. B. Greytak, G. Zheng, C. M. Lieber, *Science* **2006**, *313*, 1100.
[8] G. T. A. Kovacs, C. W. Storment, M. Halks-Miller, C. R. Belczynski, Jr., C. C. D. Santina, E. R. Lewis, N. I. Maluf, *IEEE Trans. Biomed. Eng.* **1994**, *41*, 567.
[9] P. K. Campbell, K. E. Jones, R. A. Normann, *Biomed. Sci. Instrum.* **1990**, *26*, 161.
[10] L. B. Merabet, J. F. Rizzo, A. Amedi, D. C. Somers, A. Pascual-Leone, *Nat. Rev. Neurosci.* **2005**, *6*, 71.
[11] M. A. Lebedev, M. A. L. Nicolelis, *Trends Neurosci.* **2006**, *29*, 536.
[12] K. C. Cheung, P. Renaud, H. Tanila, K. Djupsund, *Biosens. Bioelectron.* **2007**, *22*, 1783.
[13] D. Pellinen, T. Moon, R. Vetter, R. Miriani, D. Kipke, *Conf. Proc. IEEE Eng. Med. Biol. Soc.* **2005**, *5*, 5272.
[14] W. Jensen, K. Yoshida, U. G. Hofmann, *IEEE Trans. Biomed. Eng.* **2006**, *53*, 934.
[15] T. Stieglitz, H. Beutel, J. U. Meyer, *Sens. Actuators A* **1997**, *60*, 240.
[16] S. Takeuchi, T. Suzuki, K. Mabuchi, H. Fujita, *J. Micromech. Microeng.* **2004**, *14*, 104.
[17] S. Ijima, *Nature* **1991**, *354*, 56.
[18] J. Li, H. T. Ng, A. Cassell, W. Fan, H. Chen, Q. Ye, J. Koehne, J. Han, M. Meyyappan, *Nano Lett.* **2003**, *3*, 597.
[19] M. K. Yeh, N. H. Tai, J. H. Liu, *Carbon* **2006**, *44*, 1.
[20] C. E. Banks, T. J. Davies, G. G. Wildgoose, R. G. Compton, *Chem. Commun.* **2005**, 829.
[21] J. J. Gooding, *Electrochim. Acta* **2005**, *50*, 3049.
[22] V. Lovat, D. Pantarotto, L. Lagostena, B. Cacciari, M. Grandolfo, M. Righi, G. Spalluto, M. Prato, L. Ballerini, *Nano Lett.* **2005**, *5*, 1107.
[23] E. W. Keefer, B. R. Botterman, M. I. Romero, A. F. Rossi, G. W. Gross, *Nat. Nanotechnol.* **2008**, *3*, 434.
[24] M. K. Gheith, T. C. Pappas, A. V. Liopo, V. A. Sinani, B. S. Shim, M. Motamedi, J. P. Wicksted, N. A. Kotov, *Adv. Mater.* **2006**, *18*, 2975.
[25] T. D. B. Nguyen-Vu, H. Chen, A. M. Cassell, R. Andrews, M. Meyyappan, J. Li, *Small* **2006**, *2*, 89.
[26] J. Li, J. E. Koehne, A. M. Cassell, H. Chen, H. T. Ng, Q. Ye, W. Fan, J. Han, M. Meyyappan, *Electroanalysis* **2005**, *17*, 15.
[27] S. Yang, J. Huo, H. Song, X. Chen, *Electrochim. Acta* **2008**, *53*, 2238.
[28] K. Wang, H. A. Fishman, H. Dai, J. S. Harris, *Nano Lett.* **2006**, *6*, 2043.
[29] N. I. Kovtyukhova, T. E. Mallouk, L. Pan, E. C. Dickey, *J. Am. Chem. Soc.* **2003**, *125*, 9761.
[30] A. Felten, C. Bittencourt, J. J. Pireaux, G. Van Lier, J. C. Charlier, *J. Appl. Phys.* **2005**, *98*, 074308.
[31] M. Liu, Y. Yang, T. Zhu, Z. Liu, *Carbon* **2005**, *43*, 1470.
[32] T. I. T. Okpalugo, P. Papakonstantinou, H. Murphy, J. Mclaughlin, N. M. D. Brown, *Carbon* **2005**, *43*, 153.
[33] J. Kong, N. Franklin, C. Zhou, M. Chapline, S. Peng, K. Cho, H. Dai, *Science* **2000**, *287*, 622.
[34] E. Snow, F. Perkins, E. Houser, S. Badescu, T. Reinecke, *Science* **2005**, *307*, 1942.
[35] V. Toncheva, M. A. Wolfert, P. R. Dash, D. Oupicky, K. Ulbrich, L. W. Seymour, E. H. Schacht, *Biochim. Biophys. Acta* **1998**, *1380*, 354.
[36] G. L. Kenausis, J. Vörös, D. L. Elbert, N. Huang, R. Hofer, L. Ruiz-Taylor, M. Textor, J. A. Hubbell, N. D. Spencer, *J. Phys. Chem. B* **2000**, *104*, 3298.
[37] J. S. Choi, D. K. Joo, C. H. Kim, K. Kim, J. S. Park, *J. Am. Chem. Soc.* **2000**, *122*, 474.
[38] E. M. Schmidt, J. S. Mcintosh, M. J. Bak, *Med. Biol. Eng. Comput.* **1998**, *26*, 96.
[39] S. R. Yeh, Y. C. Chen, H. C. Su, T. R. Yew, H. H. Kao, Y. T. Lee, T. A. Liu, H. Chen, Y. C. Chang, P. Chang, H. Chen, *Langmuir* **2009**, *25*, 7718.
[40] S. H. Tseng, L. Y. Tsai, S. R. Yeh, *J. Neurosci.* **2008**, *28*, 7165.